

## Electronic configuration of samarium sulphide and related compounds: Mössbauer-effect measurements and a model

J. M. D. Coey, S. K. Ghatak, and M. Avignon

*Groupe des Transitions de Phases, Centre National de la Recherche Scientifique, B.P. 166X, 38042-Grenoble, France*

F. Holtzberg

*Centre des Recherches sur les Très Basses Températures, Centre National de la Recherche Scientifique, B.P. 166X, Grenoble, France*

*and I.B.M. Thomas J. Watson Research Center, Yorktown Heights, New York 10598\**

(Received 15 January 1976)

$^{149}\text{Sm}$  Mössbauer spectra have been measured at room temperature for  $\text{SmS}$  under applied pressures  $P = 0$ –11 kbar and for  $\text{Sm}_{1-x}\text{Y}_x\text{S}$ ,  $0 \leq x \leq 0.34$ . There is a sharp increase in isomer shift at  $P = 6$  kbar and  $x = 0.15$ , respectively, accompanying the transformation from the black to the gold phase, but there is no corresponding increase in linewidth. The samarium configuration, assumed to be a mixture of  $4f^6$  and  $4f^5 5d^1$ , is deduced as a function of  $P$  or  $x$ . The results suggest that the  $5d$  electron in the intermediate valence configuration is rather localized, but they are insensitive to whether the lattice is rigid or relaxed. Any fluctuations between the two configurations are more rapid than  $10^{-9}$  sec. Calculations have been made with a Falicov Hamiltonian in which a term for  $4f$ - $5d$  hybridization is included. The model accounts for the observed variations of the samarium electron configuration. It is demonstrated, both theoretically and experimentally, that yttrium doping is not simply equivalent to pressure.

### I. INTRODUCTION

In the great majority of rare-earth compounds and alloys the  $4f$  shell contains an integral number of electrons. The  $4f$  electrons are localized and highly correlated in an inner shell, hence their electronic properties are those of the rare-earth ion whose valence is its positive charge after any  $5d$  or  $6s$  conduction electrons have been removed. Typically, the rare-earths are trivalent, with a core configuration  $4f^n$ ,  $n = Z - 57$ , but some elements can also be di- or quadrivalent.

Some exceptions to this picture, cerium metal<sup>1</sup> and samarium hexaboride,<sup>2</sup> have been known for a long time. The more recent discovery of other exceptional materials, the samarium<sup>3</sup> and thulium<sup>4</sup> monochalcogenides and europium<sup>5</sup> and ytterbium<sup>6</sup> intermetallic compounds, have led to a wave of intense experimental<sup>5-15</sup> and theoretical<sup>16-24</sup> interest in the problem of valence instability in the rare earths. It seems that the problem only arises for those elements which can exhibit different valencies in different compounds. Two electronic configurations, with a difference of one in  $4f$  occupancy, must be close in energy. Normally the valency, whether  $2^+$ ,  $3^+$ , or  $4^+$ , is determined from the magnetic or optical properties of the rare-earth ion, or else from the lattice parameters of the compound. Because of the strong shielding of the outer  $5s$  and  $5p$  electrons from the nucleus by the  $4f$  shell, the addition of a  $4f$  electron increases the ionic radius. For example  $\text{Sm}^{2+}$  ( $4f^6$ ) has an ionic radius almost 20% greater

than  $\text{Sm}^{3+}$  ( $4f^5$ ). Compounds where the rare earth has an intermediate or unstable valency can be identified by their intermediate lattice parameters,<sup>12,14</sup> or else by unusual electronic properties—giant electronic specific heat,<sup>25</sup> giant Pauli-like susceptibility<sup>6,26</sup> suggestive of a very narrow  $4f$  band. The puzzle is to understand why the  $4f$  electrons seem to behave as if they were delocalized in a narrow band, despite the enormous correlation energy among them ( $U \sim 7$  eV), and the extremely small  $f$ - $f$  overlap.

Key information to be derived experimentally concerns the average electronic configuration of the rare earth, and its time dependence. Measurements of the lattice parameters,<sup>3,12,14</sup> magnetic susceptibility,<sup>6,26</sup> photoemission,<sup>4,7-9</sup> and Mössbauer spectra<sup>5,27</sup> have all been used to help determine the electronic configuration in compounds with valence instability. Each measurement possesses a different characteristic time.

The Mössbauer technique is particularly appropriate as it is a microscopic measurement which entails a negligible perturbation of the electronic system, the configuration being observed via its hyperfine interactions with the nucleus. The effect on the hyperfine interactions of electrons in different shells can be evaluated quantitatively, and the measurement can be made under pressure, if necessary. Previous work on  $\text{SmB}_6$  using the  $^{149}\text{Sm}$  resonance showed that the samarium configuration was independent of temperature and allowed an estimate of the  $\text{Sm}^{2+}/\text{Sm}^{3+}$  ratio.<sup>27</sup> A number of europium intermetallic compounds

have been studied using  $^{151}\text{Eu}$ , and some temperature dependence of the  $\text{Eu}^{2+}/\text{Eu}^{3+}$  ratio was discovered.<sup>5</sup>

As essentially only a single resonance was observed, it follows that any fluctuations are much faster than the characteristic time of the measurement. The same conclusion was reached in a preliminary study of  $\text{TmSe}$  below its magnetic ordering temperature, using the  $^{169}\text{Tm}$  resonance.<sup>15</sup>

The work reported here is a Mossbauer effect study of  $\text{SmS}$  as a function of pressure (0–11 kbar) and of  $\text{Sm}_{1-x}\text{Y}_x\text{S}$  as a function of  $x$  ( $0 \leq x \leq 0.34$ ). In  $\text{SmS}$ , the samarium undergoes a transition from a divalent black phase to a gold phase with an intermediate configuration at a pressure of about 6 kbar.<sup>3</sup> A similar transformation occurs in mixed crystals with a trivalent rare earth or yttrium sulphide<sup>12,14</sup> at  $x \sim 0.15$ .

The aim of our work was to characterize the electronic configuration in these compounds in their intermediate valence phase as fully as possible, and to achieve some insight into why the transitions occur. A preliminary account of some of the pressure results has already been published.<sup>28</sup> The results are all interpreted using a model which allows for hybridization between  $4f$  and conduction-band states.<sup>23</sup> The model has previously been used to account for the  $P$ - $V$  curves of  $\text{SmS}$ ,  $\text{SmSe}$ , and  $\text{SmTe}$ , and to predict some elastic properties of these compounds.<sup>29</sup>

## II. EXPERIMENTAL RESULTS

Six single crystals in the solid solution system  $\text{Sm}_{1-x}\text{Y}_x\text{S}$ ,  $0 \leq x \leq 0.34$ , were studied. They were prepared by slow cooling of the melt in sealed tungsten crucibles,<sup>12</sup> and were ground to a fine powder for the Mössbauer measurements. All spectra were taken at room temperature and 20  $\text{mg}/\text{cm}^2$  of the powder were mounted directly in a hermetic sample holder for the measurement of spectra at atmospheric pressure. For the measurements under pressure, the  $\text{SmS}$  powder was set in a Lucite disk 1 mm thick, and mounted between two boron carbide cylinders in the specially constructed clamp device illustrated in Fig. 1. The main requirement was that a sufficient flux of  $\gamma$  photons from the source should arrive at the detector after passing through the  $\text{SmS}$  absorber. This was achieved by a compact design which did not excessively limit the solid angle subtended by the source at the detector, and windows which transmitted a reasonable fraction (25%) of the  $\gamma$  rays emitted. Force was applied in a press onto the surface  $a$ , and the nut  $b$  was tightly screwed down. At the end of the measurement the clamp

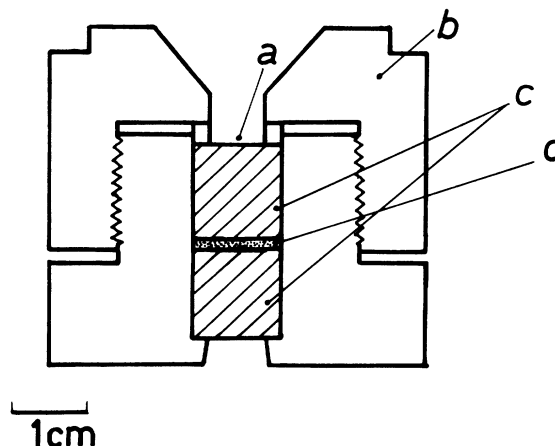


FIG. 1. Clamp used for measuring Mössbauer spectra under pressure. Details are given in the text.

was replaced in the press, and sufficient force was applied (about 10% less than before) to allow the nut to be unscrewed. The pressure was simply calculated from the average of the two forces. A pressure of about 6 kbar was needed for the transition in  $\text{SmS}$  (Fig. 3), in accord with the established value.<sup>3</sup>

The source of the  $^{149}\text{Sm}$  Mössbauer effect was  $^{149}\text{Eu}$  prepared from  $^{149}\text{Sm}$  by a  $(p, n)$  reaction, and incorporated into a matrix of  $\text{EuF}_3$ .<sup>30</sup> The initial activity of the source, which has a 106-d lifetime, was 11.5 mCi. Spectra of reasonable

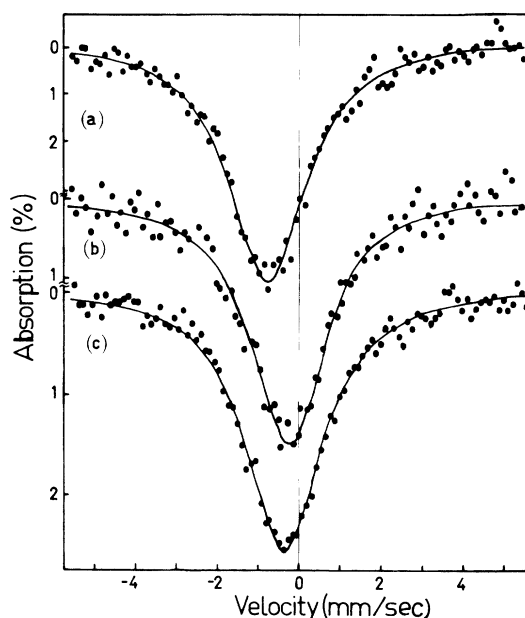


FIG. 2. Room-temperature  $^{149}\text{Sm}$  Mössbauer spectra of (a)  $\text{SmS}$  at atmospheric pressure, (b)  $\text{SmS}$  at 11 kbar, and (c)  $\text{Sm}_{0.77}\text{Y}_{0.23}\text{S}$  at atmospheric pressure.

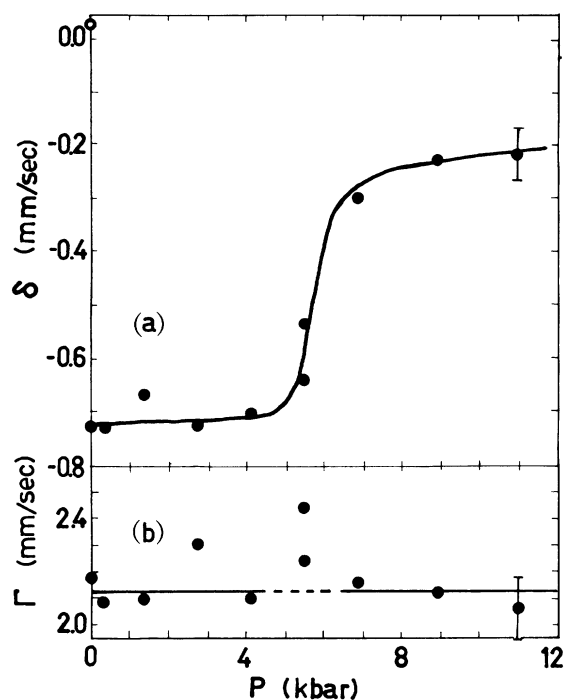


FIG. 3. (a) Isomer shift and (b) linewidth of the  $^{149}\text{Sm}$  resonance in  $\text{SmS}$  as a function of pressure.

quality could be obtained in one or two days at normal pressure, but almost a week was necessary for a good high-pressure spectrum owing to the low count rate ( $\sim 40$  counts/sec) through the clamp.

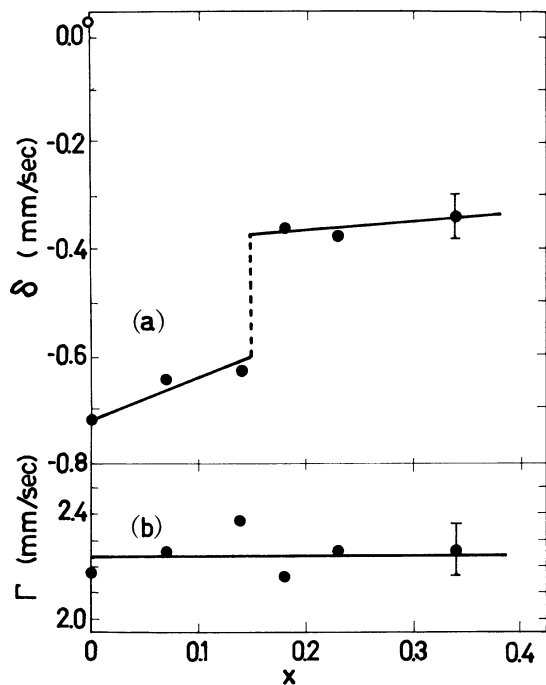


FIG. 4. (a) Isomer shift and (b) linewidth of the  $^{149}\text{Sm}$  resonance in  $\text{Sm}_{1-x}\text{Y}_x\text{S}$ .

TABLE I.  $^{149}\text{Sm}$  isomer shifts and linewidths.

	$\delta$ (mm/sec)	$\Gamma$ (mm/sec)	References
$\text{Sm}^{3+}$			
$\text{SmF}_3$	0.01(2) 0.00(6)	2.15(10) ...	a b
$\text{SmCl}_3$	-0.01(4)	2.66(16)	c
$\text{Sm}_2\text{O}_3(m)$	0.04(2) 0.01(6)	2.70(12)	c b
$\text{Sm}_2\text{S}_3$	0.03(4) 0.03(6)	3.66(20) ...	b b
$\text{Sm}_2\text{Se}_3$	-0.02(3)	2.56(12)	a
$\text{Sm}_2\text{Te}_3$	-0.10(6)	3.60(20)	a
$\text{SmN}$	0.07(2)	2.45(10)	c
$\text{SmP}$	0.04(2)	2.24(10)	a
$\text{SmAs}$	0.06(4)	2.58(16)	a
$\text{SmSb}$	0.00(4)	2.42(16)	a
$\text{Sm}$	0.25(4) 0.30(4)	2.32(15) ...	c b
$\text{Sm}^{2+}$			
$\text{SmF}_2$	0.90(4)	...	b
$\text{SmCl}_2$	-0.7	...	d
$\text{SmS}$	-0.72(2) -0.72(6)	2.24(8) ...	a b
$\text{SmSe}$	-0.71(3) -0.68(8)	2.15(12) ...	a b
$\text{SmTe}$	-0.72(4) -0.60(8)	3.04(16) ...	a b
$\text{Sm}^{2+/3+}$			
$\text{SmB}_6$	-0.33(2) -0.40(4)	1.15(8)	a b, e
$\text{Sm}_3\text{S}_4$	-0.19(4)		b

<sup>a</sup> This work. Isomer shifts are given relative to the source,  $^{149}\text{Eu}$  in  $\text{EuF}_3$ .

<sup>b</sup> Reference 35.

<sup>c</sup> Reference 31.

<sup>d</sup> Reference 33.

<sup>e</sup> Reference 27.

The 22.5-keV x rays were detected using a  $\text{Si Li}$  detector. Typical data are shown in Fig. 2.

The natural linewidth of the 22.5-keV transition is 1.71 mm/sec, and our best experimental linewidths were in the range 2.1–2.3 mm/sec.<sup>31</sup> They are narrower than those previously obtained with oxide sources,<sup>32–35</sup> and the remaining broadening could be due to paramagnetic hyperfine effects, or unresolved quadrupole interactions. All spectra were least-squares fitted to a single Lorentzian

line, and the resulting isomer shifts and line-widths for SmS as a function of pressure are plotted in Fig. 3 and for  $\text{Sm}_{1-x}\text{Y}_x\text{S}$  as a function of  $x$  are plotted in Fig. 4. A decrease in absorption area of  $(25 \pm 15)\%$  was found on passing from the black to the gold phase. Data on some other samarium compounds which will be used for comparison are collected in Table I.

### III. INTERPRETATION

First we will discuss the data of Figs. 3 and 4 in terms of configuration fluctuations. Later we will relate the results to other models for valence instability.

According to the interconfigurational fluctuation model, two electronic configurations for the rare earth are degenerate in energy, and the ion switches rapidly back and forth between the two. Following much of the earlier work,<sup>26</sup> we take the two configurations to be  $4f^6$  and  $4f^55d^1$ . The average electronic configuration of the samarium is thus

$$n_h(4f^55d^1) + (1 - n_h)(4f^6). \quad (1)$$

In general, the metallic configuration may also have some 6s character. However, the bottom of the conduction band in rare-earth metals and intermetallic compounds<sup>36</sup> has considerable 5d character. That this will be even more marked in the chalcogenides owing to the influence of the ligand field which stabilizes the  $5d(t_{2g})$  orbitals has been demonstrated by optical measurements<sup>37-39</sup> and band-structure calculations.<sup>40</sup> It is therefore reasonable to neglect the 6s character in the metallic configuration. However, it remains to be seen to what extent the 5d electron is delocalized.

From the isomer shift we can deduce the relative occupation of the two configurations. From the linewidth we can derive some information about the time associated with the configuration fluctuations. We will discuss the fluctuation time first.

The fluctuation time  $\tau$  cannot be slow compared with the characteristic time of the measurement. If it were, the spectrum in the intermediate valence state would be the superposition of absorption lines due to  $\text{Sm}^{2+}$  and  $\text{Sm}^{3+}$ , separated by no less than 0.6 mm/sec (see Table I). This would provoke an increase in linewidth in the mixed phase of approximately the same magnitude. There is no trace of line broadening in the data of Fig. 3 or 4, except perhaps for one point at 5.5 kbar, where inhomogeneity of the pressure leads to the co-existence of the divalent and mixed phases. Furthermore, fitting the spectra for  $P > 6$  kbar or  $x > 0.15$  to two Lorentzian lines of equal widths centered at  $-0.7$  and  $0.0$  mm/sec led to greater

values of  $\chi^2$  than the single-line fits. To be more precise, the increased linewidth in the mixed phase in the presence of fast fluctuations is given by<sup>5</sup>

$$\Delta\Gamma = (\pi\tau c/\hbar E_\gamma)[\delta(4f^6) - \delta(4f^55d)]^2[1 - (1 - 2n_h)^2],$$

where  $\delta$  and  $\Delta\Gamma$  are in units of mm/sec.  $E_\gamma$  is the  $\gamma$ -ray energy.

Experimentally, we find  $\Delta\Gamma \leq 0.1$  mm/sec in the high-pressure phase. The square bracket is  $\sim 0.6$  mm/sec and  $n_h \sim 0.7$ . Hence the configuration fluctuation time  $\tau \leq 10^{-9}$  sec. In the mixed crystals with  $x > 0.15$ ,  $\Delta\Gamma \leq 0.2$  mm/sec. Some line broadening may be expected because of the chemical disorder, but in any case the conclusion concerning  $\tau$  is much the same.

To evaluate the electronic configuration in the mixed phase accurately, we need to know the change in isomer shift caused by changes in 4f and 5d electron character. There is little sign of  $\text{Sm}^{3+}$  in the lattice of SmS at normal pressures,<sup>8,10</sup> so the electronic configuration of the samarium is essentially  $4f^6$ . In  $\text{Sm}_2\text{S}_3$  it is essentially  $4f^5$ . From their respective isomer shifts,  $-0.72$  and  $+0.03$  mm/sec, we deduce  $\partial\delta/\partial n_{4f} = -0.75$  mm/sec. In fact, there will be some influence of covalency and overlap distortion on the isomer shift, but the first, at least, should be much the same for the two sulphides. The 5d term is best deduced from recent results on  $^{155}\text{Gd}$ .<sup>41</sup> Some Gd impurities in  $\text{CaF}_2$  were found to be divalent ( $4f^75d^1$ ), and some trivalent ( $4f^7$ ). The difference in isomer shift reported is equivalent to  $-0.20$  mm/sec for  $^{149}\text{Sm}$ , taking the ratio of the nuclear parameter  $\Delta\langle R^2 \rangle$  for the two isotopes as  $-6.5$ .<sup>31</sup> Thus  $\partial\delta/\partial n_{5d(10c)} = -0.20$  mm/sec for a localized 5d electron. For a delocalized 5d electron the effect will be smaller. Both  $\partial\delta/\partial n_{5d(10c)}$  and  $\partial\delta/\partial n_{6s}$  have been deduced from Hartree-Fock calculations.<sup>35,41</sup> The former value agrees with the one given above, and the latter value is  $+0.45$  mm/sec. The value of  $\partial\delta/\partial n_{5d(\text{deloc})}$  can then be derived as  $-0.10$  mm/sec from the isomer shift of Sm metal assuming an electronic configuration of  $4f^55d^26s^1$ .<sup>42</sup> The numbers are collected in Table II. The value of  $n_h$  may now be calculated. If the phonon frequencies are greater than the interconfigurational fluctuation frequencies, the lattice is relaxed, and each

TABLE II. Variation of the  $^{149}\text{Sm}$  isomer shift.

Type of electron $n$	Change (mm/sec) $\partial\delta/\partial n$
4f (localized)	-0.75
5d (localized)	-0.20
5d (delocalized)	-0.10
6s (delocalized)	+0.45

samarium ion whether 2+ or 3+ occupies its normal volume. Then  $\delta$  is simply given as

$$\delta = \delta(4f^6) + n_h \left( \frac{\partial \delta}{\partial n_{5d}} - \frac{\partial \delta}{\partial n_{4f}} \right). \quad (2)$$

If, on the other hand, the lattice does not respond to the electronic configuration fluctuations, we must add a volume correction. The rigid lattice is equivalent to a positive pressure on  $\text{Sm}^{2+}$  and a negative pressure on  $\text{Sm}^{3+}$ :

$$d\delta = \left( \frac{\partial \delta}{\partial n_h} \right)_V dn_h + \left( \frac{\partial \delta}{\partial V} \right)_{n_h} dV. \quad (3)$$

The volume correction can be estimated from extensive studies of the volume dependence of the isomer shift of  $^{153}\text{Eu}$ . It is found that the isomer-shift change has almost exactly the same linear dependence on the reduced volume change for a

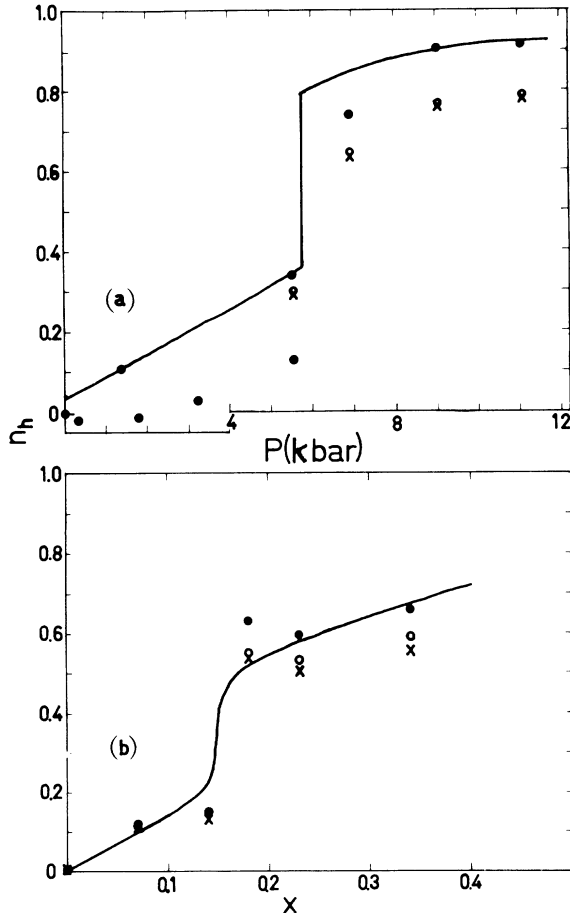


FIG. 5. Fraction of  $\text{Sm}^{3+}$  in (a)  $\text{SmS}$  as a function of pressure and (b)  $\text{Sm}_{1-x}\text{Y}_x\text{S}$ . The isomer shifts of Figs. 3 and 4 have been interpreted assuming delocalized  $5d$  electrons and a rigid lattice ( $\times$ ); delocalized  $5d$  electrons and a relaxed lattice ( $\circ$ ); localized  $5d$  electrons and a rigid lattice ( $\bullet$ ).

number of insulating and metallic compounds of divalent and trivalent europium.<sup>43</sup> Transposition of the results to  $\text{SmS}$ , using a ratio of  $\Delta(R^2)$  for  $^{149}\text{Sm}$  and  $^{153}\text{Eu}$  of  $-90$ , we deduce  $(\partial\delta/\partial V)_{n_h} = -0.0013$   $\text{mm}/\text{sec}/\text{\AA}^3$ . The slight volume dependence of the isomer shift is illustrated in Fig. 7 by a dotted line.

The values  $n_h$  deduced from Eq. (2) are shown in Fig. 5. The solid dots correspond to localized  $d$  electrons and the crosses to delocalized ones. The open dots show the effect of the volume correction of Eq. (3) in the latter case. The electronic configuration derived from the isomer shift is therefore quite sensitive to the hypothesis made concerning the localization of the  $d$  electrons, but it is quite insensitive to whether the lattice can follow the configuration fluctuations or not.

In the samarium-yttrium mixed crystals, the configuration deduced will be changed by an insignificant amount ( $<0.02$ ) if we take a common Sm-Y  $d$  band instead of the separate samarium  $5d$  band assumed here. The trivalent character in the gold phase is in any case smaller than in the pure material under pressure.

Finally, we comment on the valence of samarium in the pnictides. The isomer shifts (Table I) fall squarely in the range for trivalent samarium. The decrease in isomer shift as one goes down the series is also found in the trivalent 2:3 chalcogenides. It may be due to an increase in the ratio of  $5d/6s$  character in the antibonding orbitals (or conduction band) resulting from the lowering of the  $5d(t_{2g})$  level by the ligand field.

#### IV. MODEL

To account for the abrupt changes in the electronic configuration of  $\text{SmS}$  as a function of pressure or yttrium doping, we will apply a model to the problem which was first used by Falicov *et al.*<sup>44</sup> to explain the behavior of certain transition-metal oxides. The essential feature of the model is the simultaneous presence of interacting localized ( $4f$ ) and extended ( $5d$ ) band states. We showed previously<sup>23</sup> how the giant electronic specific heat of  $\text{SmS}$  in its high-pressure phase could be explained provided that hybridization between the localized and extended states was included. The difference in nature of the transition in  $\text{SmS}$  on the one hand and  $\text{SmSe}$  and  $\text{SmTe}$  on the other could also be obtained. The Hamiltonian is

$$\begin{aligned} H = & \sum_{\mathbf{k}} E(\mathbf{k}) a_{\mathbf{k}}^{\dagger} a_{\mathbf{k}} + E_0 \sum_i b_i^{\dagger} b_i \\ & - G \sum_i b_i^{\dagger} a_i^{\dagger} a_i b_i \\ & - \sum_{i, \mathbf{k}} V_{ki} (a_{\mathbf{k}}^{\dagger} b_i^{\dagger} + a_{\mathbf{k}} b_i). \end{aligned} \quad (4)$$

$a_k^\dagger(a_k)$ ,  $b_i^\dagger(b_i)$  are the usual creation (destruction) operators for electrons in the band and holes in localized states, respectively. The first term represents the energy of the electrons in the  $d$  band; the second term is the energy necessary to create ions in the  $4f^5$  configuration from ions in the  $4f^6$ . The third term describes the electron-ion interaction, where  $G$  is the difference in energy of the  $d$  orbitals in the presence of a  $4f^6$  or  $4f^5$  core. Hybridization between localized and band states is described by the last term.

This Hamiltonian was solved in the Hartree-Fock approximation, treating the system as a collection of independent impurities. The density of states is Lorentzian:

$$D_{4f}(E) = \{\epsilon(E)/[\epsilon^2(E) + (E - Gn_e)^2]\}. \quad (5)$$

$E_0$  is taken as the energy reference and  $n_e$  is the average number of a conduction electrons per atom. The half-width is a function of the position of the  $4f$  level:

$$\epsilon(E) = \sum_k |V_{ki}|^2 \delta(E - E(k)) \quad (6)$$

and it changes discontinuously as soon as the  $4f$  level enters the conduction band, giving a transition which will always be discontinuous.<sup>17</sup> There is therefore no means of distinguishing the behavior of SmS (discontinuous change of the electronic configuration under pressure) from SmSe or SmTe (continuous change). This difficulty may be avoided by replacing  $\epsilon(E)$  by a constant  $\epsilon$  independent of energy.<sup>23</sup> The model band scheme is illustrated in Fig. 6. In this one-electron picture the

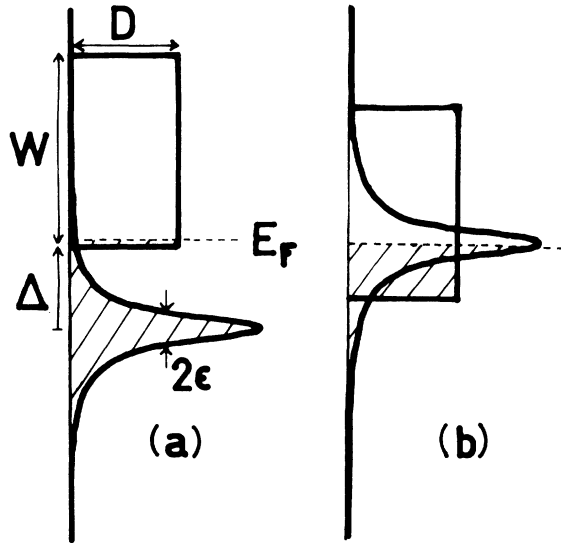


FIG. 6. Schematic one-electron band scheme used in the calculations. (a) The black phase and (b) the gold phase of SmS or  $\text{Sm}_{1-x}\text{Y}_x\text{S}$ .

broadened  $4f$  level represents the density of states of the sixth  $4f$  electron moving in the field of the  $4f^5$  ion cores.

The average number of holes (Sm<sup>3+</sup> ions) in the localized level at finite temperature is found by using Fermi statistics and integrating over the whole energy scale:

$$n_h = \frac{1}{2} \text{Im} \Psi \left( \frac{1}{2} + \frac{\epsilon}{2\pi kT} - \frac{i(E_F - Gn_e)}{2\pi kT} \right), \quad (7)$$

where  $\Psi(z)$  is the complex digamma function.

The average number of electrons in the band is given by the equation

$$n_e = \int \frac{D(E)dE}{1 + \exp[(E - E_F)/kT]}, \quad (8)$$

where  $D(E)$  is the density of states of the band. Let  $D^0(E)$  be the original density of states of conduction electrons assumed to be a constant  $D$  for  $\Delta < E < \Delta + W$  and zero elsewhere (Fig. 6). As a consequence of the mean-field approximation, the band moves rigidly when  $4f$  electrons from Sm<sup>2+</sup> ions are excited into it, and  $D(E) = D^0(E + Gn_h)$ . The Fermi energy is determined by the condition  $n_e = n_h$  in pure SmS, but in the mixed crystals with a joint  $d$  band by

$$n_e = (1 - x)n_h + x. \quad (9)$$

With the above assumptions, and when  $W \gg kT$ , the Fermi energy is given

$$E_F = \Delta - Gn_h(1 - x) + n_e/D + kT \ln(1 - e^{-n_e/DkT}). \quad (10)$$

Equations (7)–(10) are a set which are to be solved self-consistently for  $n_h$ .

The problem has now been parametrized in terms of  $\Delta$ ,  $D$ , and  $\epsilon$ . An appropriate choice will give either a continuous or a discontinuous transition. The continuous curve in Fig. 5(a) has been calculated using  $\Delta = 65$  meV,<sup>45</sup>  $\partial\Delta/\partial P = -10$  meV/kbar,  $\epsilon = 5$  meV, and  $X [= (1/D - 2G)/\epsilon] = -6$ . The first two values are measured values while the latter two are adjustable parameters. For the yttrium-doped samples we suppose  $\partial\Delta/\partial x = -400$  meV and a density of states  $D = (1 - x)D(\text{SmS}) + xD(\text{YS})$ , with  $D(\text{SmS}) = 4$  states/eV and  $D(\text{YS}) = 2.2$  states/eV. Taking the other parameters to be the same as for pure SmS we calculate the solid line of Fig. 5(b).

In a general way we see from the model that yttrium doping is not simply the equivalent of pressure. Besides the reduction of lattice volume, there are two other effects of yttrium doping. The  $d$  electron brought by each yttrium ion tends to raise the Fermi level, and so helps to stabilize the black phase. The position of the bottom of the joint conduction band and its density of states also

plays a role. Finally, we mention that if it were too far above the  $4f$  level, no transition could occur at all [cf.  $(\text{Sm}_{1-x}\text{Ca}_x)\text{S}$ ].<sup>46</sup>

### V. DISCUSSION

In Sec. III the experimental results were considered in terms of configuration fluctuations. However there is nothing in the results which implies that such an approach is necessarily valid. All we can conclude is that if fluctuations between two well-defined electronic configurations are occurring, then they must be more rapid than  $10^{-9}$  sec. We can rule out the possibility of a static or slowly fluctuating random distribution of  $\text{Sm}^{2+}$  and  $\text{Sm}^{3+}$  ions. In x-ray photoemission spectra on mixed  $(\text{Sm}_{1-x}\text{R}_x^{3+})\text{S}$  crystals, well-defined structure has been identified with the daughter  $4f^4$  and  $4f^5$  configurations.<sup>8,9</sup> If the strong perturbation of the electronic system needed to make the measurement can safely be ignored, then the fluctuation time must be less than about  $10^{-15}$  sec, the characteristic time of the measurement. Hence  $10^{-9} \geq \tau \geq 10^{-15}$  sec. These are generous limits, and correspond in terms of energy to  $10^{-6} \leq \epsilon \leq 1$  eV. The separation of the  $4f^6$  and  $4f^5 5d^1$  levels must fall within these limits.<sup>16</sup>

From the point of view of a virtual bound state, or a narrow  $4f$  band, the lifetime of a particular electronic configuration is given by the width of the bound state or the bandwidth. Not only a conduction band, but any hybridized atomic orbital will exhibit spontaneous fluctuations of the atomic electronic configuration. Such fluctuations are essential for metallic conduction, as well as for superexchange. In terms of our model, the width  $\epsilon = 5$  meV of the  $4f$  level, corresponds to a configuration lifetime of  $\sim 10^{-13}$  sec. In this context, the magnetic susceptibility at low temperatures may be understood as a narrow-band Pauli susceptibility. Such a susceptibility occurs when the configuration fluctuation time becomes shorter than the spin-lattice relaxation time, so the Boltzmann population of the Zeeman levels necessary for Curie-Weiss susceptibility cannot be established. The spin-lattice relaxation time itself increases rapidly with decreasing temperature and we expect that it is longer than  $10^{-13}$  sec in  $\text{SmS}$ . In certain trivalent samarium salts for example, paramagnetic hyperfine structure is observed in Mössbauer spectra at 4.2 K,<sup>47</sup> which implies that the relaxation time for the  $\text{Sm}^{3+}$  ion exceeds  $10^{-9}$  sec. Our experimental results would also be quite consistent with an excitonic-type state which has been suggested recently.<sup>48</sup> The data for  $0 \leq x \leq 0.15$  in Fig. 4 suggest that there is some trivalent samarium already present in the black phase though the data on  $\text{SmS}$  below 6 kbar

are equivocal on this basis. Nevertheless, the tendency for  $n_h$  to increase with  $x$  in this range is also well reproduced by our model. The black color might then be explained by a plasma frequency in the infrared region due to the small number of carriers.

In Fig. 7 we plot the isomer shifts for  $\text{SmS}$  and  $\text{Sm}_{1-x}\text{Y}_x\text{S}$  as a function of cell volume. Two significant conclusions can be drawn from this diagram. In the first place, it is clear that *yttrium doping is not simply equivalent to pressure*. The two sets of points in the gold phase are separated by an amount outside the experimental errors. The difference is too great to be explained by the donation of the yttrium  $4d$  electron to the conduction band. It could however, be explained if the lattice in the mixed crystal is locally strained so that the samarium sees a volume 3% greater than the average volume. In the second place, the straight line drawn through the data as function of pressure extrapolates to  $\delta = -0.17$  at the volume corresponding to  $\text{Sm}^{3+}\text{S}$ . This is exactly the isomer shift if the  $5d$  electron is *localized*, i.e., contributes  $-0.20$  instead of  $-0.10$  mm/sec. Furthermore the theoretical curves in Fig. 5 lie closer to the experimental points interpreted in terms of localized  $5d$  electrons rather than completely delocalized ones. This suggests that the electrons promoted to the bottom of the conduction band are quite heavy

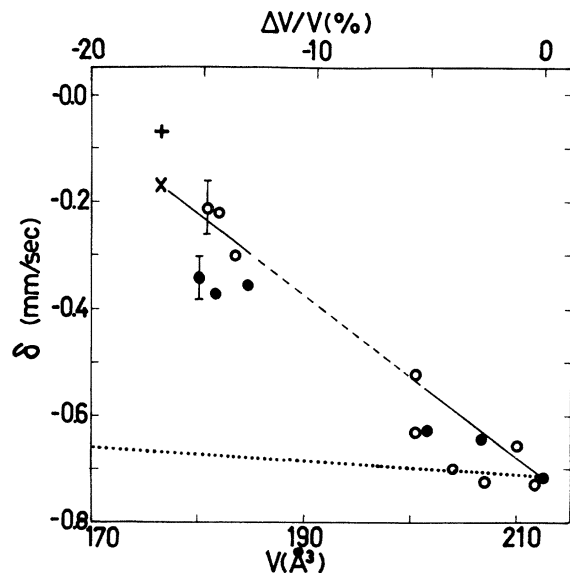


FIG. 7. Isomer shift of  $\text{SmS}$  under pressure ( $\circ$ ) and of  $\text{Sm}_{1-x}\text{Y}_x\text{S}$  ( $\bullet$ ), plotted as a function of unit cell volume. The dotted line shows the variation of isomer shift which would result if the electronic configuration of Samarium remained  $4f^6$  throughout. The points  $\times$  and  $+$  correspond to  $\text{Sm}^{3+}\text{S}$ , assuming that the  $d$  electron is localized and delocalized, respectively.

TABLE III. Comparison of the electronic configuration of samarium in the gold phase of  $\text{Sm}_{1-x}\text{Y}_x\text{S}$  determined in different ways.

Method	$x$	$n_h$
Mössbauer effect	0, 18	
5 <i>d</i> localized		0, 60
5 <i>d</i> delocalized		0, 52
Lattice parameter	0, 19	0, 70 <sup>a</sup>
X-ray photoemission	0, 19	0, 58 <sup>a</sup>

<sup>a</sup> Reference 8.

and behave like localized ones. If the *d* electrons really are rather localized, the choice of a valid model for the microscopic mechanism of the fluctuations is quite limited. The model proposed by Kaplan and Mahanti requires that the fluctuations on neighboring sites be coupled,<sup>24</sup> as may be expected from considering the strain energy.

At this point we compare our model with others that have appeared recently. The model we use is purely electronic, and explains the electronic configuration, *P-V* relation, and electronic specific heat in a coherent way, with a small number of parameters. Unlike that of Sicardi *et al.*,<sup>17</sup> ours includes the electron-hole interaction which permits us to obtain both continuous and discontinuous transitions. Other models take into account the lattice energy, whether harmonic<sup>16</sup> or anharmonic<sup>20,22</sup> and obtain transitions without invoking *G*. At present it is difficult to discern the correct driving mechanism, and both probably intervene to some extent. The electron-phonon interaction probably also helps to lower the energy of the gold phase. The decrease in absorption area of the spectrum in the gold phase suggests a decrease in Debye-Waller factor. Detailed x-ray diffraction measurements would be desirable.

Finally, we conclude with a comparison of the Mössbauer technique with the other methods that have been used to determine the electronic configuration of the rare earth in these valence-in-

stability compounds. In Table III we compare three methods which have been applied to gold yttrium-doped samples of almost identical composition. The agreement is surprisingly good, and there can be little doubt of the reality of an intermediate configuration when it is observed by three completely different methods. The advantages which Mössbauer spectroscopy possesses compared to XPS are that it introduces a negligible perturbation of the system, can be performed under pressure, and is not especially surface sensitive. Compared with the lattice-constant measurements, it permits an analysis of the contributions of different types of electrons, and does not rely on Vegard's law. Our estimate of the trivalent character in the mixed crystals is rather smaller than the one derived from the lattice parameter. Mössbauer measurements are unfortunately expensive and time consuming but good isotopes exist for Sm, Eu, and Tm, and useful results can be obtained with samarium despite its poor resolution.

## VI. CONCLUSIONS

We have shown that the characteristic time for any electronic configuration fluctuation is less than a nanosecond in the gold phases of SmS, under pressure and in  $\text{Sm}_{1-x}\text{Y}_x\text{S}$ . The intermediate valence configurations have been determined in both systems, assuming negligible 6*s* character, but the results neither confirm nor deny the configuration fluctuation picture. The samarium has less trivalent character in the gold phase of  $\text{Sm}_{1-x}\text{Y}_x\text{S}$  than of SmS under pressure. There is an indication that the 5*d* electron is rather localized in the intermediate valence state. The work on SmS is the first use of the Mössbauer effect to study a "metal-insulator" transition as a function of pressure.

We have compared our results with calculations in terms of a Falicov Hamiltonian, taking account of 4*f* – 5*d* hybridization. With three free parameters, the model gives an acceptable account of the experimental data.

\*Permanent address.

<sup>1</sup>B. Coqblin and A. Blandin, *Adv. Phys.* **17**, 281 (1968), and references therein.

<sup>2</sup>J. C. Nickerson, R. M. White, K. N. Lee, R. Backmann, T. H. Geballe, and G. W. Hull, *Phys. Rev. B* **3**, 2030 (1971), and references therein.

<sup>3</sup>A. Jayaraman, V. Narayanamurti, E. Bucher, and R. G. Maines, *Phys. Rev. Lett.* **25**, 368 (1970); **25**, 1430 (1970); A. Chattarjee, A. K. Singh, and A. Jayaraman, *Phys. Rev. B* **6**, 2285 (1972).

<sup>4</sup>M. Campagna, E. Bucher, G. K. Wertheim, P. N. E.

Buchanan, and L. D. Longinotti, *Phys. Rev. Lett.* **32**, 885 (1974).

<sup>5</sup>E. R. Bauminger, I. Felner, D. Levron, I. Nowik, and S. Ofer, *Phys. Rev. Lett.* **33**, 890 (1974); E. R. Bauminger, I. Felner, D. Freindlich, D. Levron, I. Nowik, S. Ofer, and R. Yanovsky, *J. Phys.* **35**, C6-61 (1974).

<sup>6</sup>B. C. Sales and D. Wohlleben, *Phys. Rev. Lett.* **18**, 1240 (1975).

<sup>7</sup>J. L. Freeouf, D. E. Eastman, W. D. Grobman, F. Holtzberg, and J. B. Torrance, *Phys. Rev. Lett.* **33**, 161 (1974).



- <sup>8</sup>M. Campagna, E. Bucher, G. K. Wertheim, and L. D. Longinotti, *Phys. Rev. Lett.* **33**, 165 (1974).
- <sup>9</sup>R. A. Pollak, F. Holtzberg, J. L. Freeouf, and D. E. Eastman, *Phys. Rev. Lett.* **33**, 820 (1974).
- <sup>10</sup>W. M. Walsh, E. Bucher, L. W. Rupp, and L. D. Longinotti, *AIP Conf. Proc.* **24**, 34 (1975).
- <sup>11</sup>G. Guntherot and F. Holtzberg, *AIP Conf. Proc.* **24**, 36 (1975).
- <sup>12</sup>L. J. Tao and F. Holtzberg, *Phys. Rev. B* **11**, 3842 (1975).
- <sup>13</sup>T. Penney and F. Holtzberg, *Phys. Rev. Lett.* **34**, 322 (1975).
- <sup>14</sup>A. Jayaraman, P. Dernier, and L. D. Longinotti, *Phys. Rev. B* **11**, 2783 (1975).
- <sup>15</sup>B. B. Triplett, N. S. Dixon, P. Boolchand, S. S. Hanna, and E. Bucher, *J. Phys.* **35**, C6-653 (1974).
- <sup>16</sup>L. L. Hirst, *Phys. Kondens. Mater.* **11**, 255 (1970); *J. Phys. Chem. Solids* **35**, 1285 (1974); *AIP Conf. Proc.* **24**, 11 (1975).
- <sup>17</sup>J. R. Sicardi, A. K. Bhattacharjee, R. Jullien, and B. Coqblin, *Solid State Commun.* **16**, 499 (1975).
- <sup>18</sup>H. J. Wio, B. Alascio, and A. Lopez, *Solid State Commun.* **15**, 1933 (1974).
- <sup>19</sup>N. F. Mott., *Philos. Mag.* **30**, 403 (1974).
- <sup>20</sup>P. W. Anderson and S. T. Chui, *Phys. Rev. B* **9**, 3209 (1974).
- <sup>21</sup>D. Sherrington and S. von Molnar, *Solid State Commun.* **16**, 1347 (1975).
- <sup>22</sup>C. M. Varma and V. Heine, *Phys. Rev. B* **11**, 4763 (1975).
- <sup>23</sup>M. Avignon and S. K. Ghatak, *Solid State Commun.* **16**, 1243 (1975).
- <sup>24</sup>T. A. Kaplan and S. D. Mahanti, *Phys. Lett. A* **51**, 265 (1975).
- <sup>25</sup>S. D. Bader, N. E. Phillips, and D. B. McWhan, *Phys. Rev. B* **7**, 4686 (1973).
- <sup>26</sup>M. B. Maple and D. Wohlleben, *Phys. Rev. Lett.* **27**, 511 (1971).
- <sup>27</sup>R. L. Cohen, M. Eibschütz, and K. W. West, *Phys. Rev. Lett.* **24**, 383 (1970).
- <sup>28</sup>J. M. D. Coey, S. K. Ghatak, and F. Holtzberg, *AIP Conf. Proc.* **24**, 38 (1975).
- <sup>29</sup>S. K. Ghatak, in *Phonon Scattering in Solids*, edited by L. J. Chablis *et al.* (Plenum, New York, 1976), p. 305; M. Avignon and S. K. Ghatak, *Europhysics Conf. Abstr.* **1A**, 46 (1975); and (unpublished).
- <sup>30</sup>Supplied by the New England Nuclear Corp.
- <sup>31</sup>J. M. D. Coey, *J. Inorg. Nucl. Chem.* **38**, 1139 (1976).
- <sup>32</sup>V. P. Alfimenkov, N. A. Lebedev, Y. M. Ostonevich, T. Ruskov, and A. V. Strelkov, *Soviet Physics J. E. T. P.*, **19**, 326 (1964).
- <sup>33</sup>W. Henning, G. Kaindl, P. Kierle, H. J. Komer, H. Kulzer, K. E. Rehm, and N. Edelstein, *Phys. Lett. A* **28**, 209 (1968).
- <sup>34</sup>S. Ofer, E. Segal, I. Nowik, E. R. Bauminger, L. Grodzins, A. J. Freeman, and M. S. Schieber, *Phys. Rev.* **137**, A627 (1965).
- <sup>35</sup>M. Eibschütz, R. L. Cohen, E. Buehler, and J. H. Wernick, *Phys. Rev. B* **6**, 18 (1972).
- <sup>36</sup>M. Belakhovsky and D. K. Ray, *Phys. Rev. B* **12**, 3956 (1975).
- <sup>37</sup>F. Holtzberg and J. B. Torrance, *AIP Conf. Proc.* **5**, 860 (1971); R. Suryanarayanan, C. Paparoditis, J. Ferré, and B. Briat, *J. Appl. Phys.* **43**, 4105 (1972).
- <sup>38</sup>E. Batlogg, J. Schoenes, and P. Wachter, *Phys. Lett.* **49A**, 13 (1974).
- <sup>39</sup>T. Kasuya, *Crit. Rev. Solid State Sci.* **3**, 131 (1972).
- <sup>40</sup>S. J. Cho, *Phys. Rev. B* **1**, 4589 (1970); H. L. Davis, in *Proceedings of the Ninth Rare Earth Conference* (USGPO, Washington, D. C., 1972), Vol. 1, p. 3.
- <sup>41</sup>H. A. Buskes and J. D. Cashion, *J. Phys.* **35**, C6-221 (1974).
- <sup>42</sup>J. F. Herbst, D. N. Lowy, and R. E. Watson, *Phys. Rev. B* **6**, 1913 (1972).
- <sup>43</sup>G. M. Kalvius, U. F. Klein, and G. Wortmann, *J. Phys.* **35**, C6-139 (1974).
- <sup>44</sup>L. M. Falicov, J. C. Kimball, *Phys. Rev. Lett.* **22**, 997 (1969).
- <sup>45</sup>E. Kaldis and P. Wachter, *Solid State Commun.* **11**, 907 (1972).
- <sup>46</sup>J. E. Smith, F. Holtzberg, M. I. Nathan, and J. C. Tsang (unpublished).
- <sup>47</sup>S. Ofer and I. Nowik, *Nucl. Phys. A* **93**, 689 (1967).
- <sup>48</sup>J. Schweitzer, *Phys. Rev. B* **13**, 3506 (1976); S. T. Chui, *ibid.* **13**, 2066 (1976); S. K. Ghatak, M. Avignon, and K. H. Bennemann, *J. Phys. F* (to be published).